Mesozoic Structure and Petroleum Systems in the De Soto Canyon Salt Basin in the Mobile, Pensacola, Destin Dome, and Viosca Knoll Areas of the MAFLA Shelf

Pashin, Jack C.

Boone Pickens School of Geology Oklahoma State University Stillwater, Oklahoma 74078 e-mail: jack.pashin@okstate.edu Guohai, Jin Hills, Denise J. Geological Survey of Alabama P.O. Box 869999 Tuscaloosa, Alabama 35486-6999

Abstract

Large parts of the De Soto Canyon Salt Basin are unexplored, and structural and petroleum system models may facilitate continued hydrocarbon exploration, as well as the development of geologic CO₂ storage programs. The basin contains four structural provinces: (1) Destin fault system, (2) salt pillow province, (3) diapir province, and (4) salt roller province. The Destin fault system bounds half grabens that formed near the updip limit of salt. The faults have variable displacement and were active mainly during the Cretaceous. Broad salt pillows occur basinward of the Destin fault system, and the largest of these structures forms the core of Destin Dome. Salt pillows basinward of Destin Dome began forming shortly after Smackover deposi-

tion, whereas Destin Dome largely post-dates the Destin fault system. The diapir province is in the structurally deepest part of the salt basin, and diapirism occurred from the Jurassic into the Tertiary. The salt roller province contains a complex array of normal faults and rollover structures that record gravitational shelf spreading during Jurassic time. Petroleum systems analysis indicates that the basin contains a distinctive suite of source rocks, sealing strata, reservoir strata, and trap types. Exploration efforts have thus far proven successful in structures that formed before or during hydrocarbon expulsion, and many such structures remain untested.

Introduction

The De Soto Canyon salt basin extends from offshore Mississippi to the western Florida Panhandle (the MAFLA shelf) and contains a thick succession of Mesozoic and Cenozoic strata that includes siliciclastic, carbonate, and evaporite facies (Figs. 1 and 2). The basin is part of the Gulf of Mexico continental shelf, straddling the boundary between the Central and Eastern Gulf of Mexico planning areas of the U.S. Bureau of Ocean Energy Management (BOEM). The basin contains a diverse suite of salt tectonic structures. including peripheral faults, salt pillows, salt rollers, and salt diapirs. Major hydrocarbon production has been proven in Jurassic eolianite along the northern flank of the basin, and additional potential in the Mesozoic section has been identified in Cretaceous reefs along the shelf margin (e.g., Mancini et al., 1986; Story, 1998; Petty, 1999; Montgomery et al., 2002). Nevertheless, the region remains underexplored, and no detailed petroleum systems analysis has been performed, partly because of a moratorium on drilling and production on the continental shelf in the Eastern Gulf of Mexico planning area. However, a new initiative directed at quantifying the sub-seabed CO₂ storage and CO₂enhanced hydrocarbon recovery potential of the Gulf of Mexico and Atlantic continental shelves has provided a new impetus for geological characterization of the De Soto Canyon salt basin.

The central objectives of this paper are to characterize the structural framework and Mesozoic

petroleum systems of the De Soto Canyon salt basin in the Mobile, Viosca Knoll (north), Pensacola, and Destin Dome areas (Fig. 1). This research began under the sponsorship of the U.S. Minerals Management Service (now BOEM) in 1999 and continues today with support from the U.S Department of Energy's National Energy Technology Laboratory through the Southern States Energy Board. Seismic data provide high quality imaging of salt structures in the De Soto Canyon salt basin and provide a basis for characterizing structural geometry, making balanced structural restorations, and analyzing structural chronology.

An important goal of this research was to improve understanding of the temporal and kinematic relationships among different classes of salt structures and how these relationships relate to hydrocarbon generation and entrapment. Similar suites of structures are common in other Gulf Coast salt basins, including the Mississippi Interior, Louisiana, and East Texas basins (e.g., Hughes, 1968; Martin, 1978; Jackson, 1982; Pashin et al., 1998, 2000; Pearson et al., 2012). Hence, the results of this investigation may help inform continuing geological characterization, exploration, and development efforts in the region. This paper begins with a summary of the methods used in this research and continues by discussing the stratigraphic and structural framework. The focus shifts to characterization of the structural evolution and burial and thermal history

Pashin et al. 417 ▶

of the basin, and the results are then synthesized into a petroleum systems model.

Methods

The basic materials used in this research are publically available 2D reflection seismic surveys, geophysical well logs, checkshot surveys, sample descriptions, and paleontological reports. Regionally extensive seismic reflections from the Jurassic section to the modern sea floor were identified, correlated and traced among 2D seismic profiles using Schlumberger GeoQuest software. A series of reference wells was used to tie seismic reflections to stratigraphic contacts as identified in resistivity, gamma-neutron-density, and sonic well logs. Checkshot surveys and synthetic seismograms were used to identify the precise stratigraphic positions of seismic events from the top of the Louann Salt to the sea floor and to calculate interval velocities for depth conversion of selected seismic profiles.

Key seismic profiles were interpreted using standard seismic- and sequence-stratigraphic procedures (e.g., Vail, 1987). Emphasis was placed on identifying stratal architecture and defining the relationship between stratal and structural geometry. As markers were traced, discontinuous and offset reflections, as well as oblique events connecting those discontinuities (i.e., fault-related reflections and amplitude anomalies), were used to delineate faults. Hanging-wall and footwall bed cutoffs were marked at the intersections of the seismic markers with each fault. Fault polygons were

then defined in plan view by connecting the cutoff points. Each seismic marker and fault surface was then gridded and contoured to make time structure maps. Isochron maps showing the vertical time thickness of each stratigraphic interval also were made. Depth-based structure and isochore maps also were made, although the veracity of these maps is questionable in undrilled parts of the basin, where velocity-depth relationships are less certain. Three-dimensional visualizations of key bed and fault surfaces were made using the GeoViz module of GeoQuest, and the grids were exported to ASCII files so that additional 3D visualizations and analyses could be made using 3DMove software.

To characterize structural style and evolution, selected 2D seismic profiles (Fig. 1) were used to make time-structural cross sections showing the positions of key stratigraphic markers and faults. Cross sections were depth-converted and then restored sequentially in Lithotect software using many of the techniques discussed by Rowan and Kligfield (1989). In all restorations, bed length was preserved, and strata were restored by defining fold axes and unfolding the beds using a simple-shear, flexural-slip technique. As beds were unfolded, faulted surfaces were restored by a combination of rigid-body displacement and simple shear. Extensional strain was calculated for each restoration

Pashin et al. 418 ▶

step using the methods of Groshong (1994) and Groshong *et al.* (2003). To help understand patterns of salt flow, 3D models of total effective subsidence were made by integrating time thickness and backstripped sediment thickness calculated during burial history analysis.

Burial and thermal modeling employed a series of techniques, including analysis of geothermics, thermal maturity, backstripping, Lopatin modeling, and expulsion modeling. Although no direct control on thermal maturity was available in the De Soto Canyon salt basin, maturity data published by Kopaska-Merkel and Schmoker (1994) and Carroll (1999) from onshore Alabama were used as analogs to help constrain maturitydepth relationships. Burial and thermal history were modeled using BasinMod software. Burial history was modeled using the basic methods of van Hinte (1978) and Angevine et al. (1990) for lithologic control and the time scale of Gradstein et al. (2012) for time control. Thermal maturation and hydrocarbon generation windows were modeled using the Lopatin method (Waples, 1980) for wells representing different parts of the salt basin. Geothermal gradients were controlled by modern wellbore temperatures and estimates of post-rift thermal decay. Plots of thermal maturation versus time were constructed, as were plots of hydrocarbon expulsion versus time.

Petroleum system analysis followed the basic procedures discussed by Magoon and Dow (1994). Known and potential source rocks, carrier beds, reservoir rocks, and seals were identified on the basis of stratigraphic, structural, and petrologic information. Next, these key strata were superimposed on Lopatin models to place them into context in terms of burial history, thermal maturation, and the timing of oil expulsion. Special attention was paid to the the relationship of structural chronology to the timing of thermal maturation and hydrocarbon expulsion. After this, structural and facies patterns were analyzed to characterize possible migration pathways and hydrocarbon trapping mechanisms. Finally, the results were synthesized into an integrated petroleum systems model and event chart that summarizes the controls on hydrocarbon generation, expulsion, migration, and trapping.

Stratigraphic Framework

Strata in the De Soto Canyon salt basin include siliciclastic rocks, carbonate rocks, and evaporites deposited during Triassic-Jurassic rifting and subsequent passive margin development during opening of the Gulf of Mexico. Rifting initiated a counterclockwise rotation of the Yucatan block relative to North America (e.g., Pindell and Kennan, 2001; Sandwell et al., 2014). Rift basins were filled with siliciclastic sediment of the Eagle Mills Formation, and these basins and the surrounding basement complexes were truncated by a regionally extensive breakup unconformity (Dobson and Buffler, 1991; MacRae and Watkins,

Pashin et al. 419 ▶

1995). Following unconformity development, evaporite sedimentation culminated in deposition of the Middle Jurassic Louann Salt, which locally forms diapiric bodies that extend more than 22,000 feet above basement (Figs. 2 and 3).

Above the Louann Salt, are the sandstone of the Norphlet Formation and the limestone and dolomite of the Smackover Formation. The Norphlet is dominantly an eolian unit and is in places thicker than 1,000 feet (Mancini et al., 1985; Story, 1998). In the De Soto Canyon salt basin, the Norphlet is imaged in updip regions as a series double-convex lenses (Fig. 3). The Smackover, by comparison, is composed mainly of limestone and shale and represents development of an extensive carbonate bank (Dobson and Buffler, 1997). The Smackover is draped over Norphlet sandstone bodies and contains a giant array of synsedimentary growth structures associated with salt diapirs (Fig. 3A) and rollers (Fig. 3C). Reflections in the Smackover section are subparallel to divergent and define rollover folds associated with fault-bounded Louann salt rollers. The Haynesville Formation is dominated by limestone, and the contact with the Smackover is in places indistinct. However, an angular unconformity at the base of the Haynesville is defined by discordant termini of dipping Smackover reflections (Fig. 3B) and salt rollers (Fig. 3C). The Smackover-Haynesville section is thicker than 1.2 s (> 10,000 ft) and is preserved in a giant roho structure (Fig. 3C).

The Cotton Valley Group spans the Jurassic-Cretaceous boundary and contains mainly siliciclastic rocks (Fig. 2). Reflections within the Cotton Valley Group are subparallel, although geometry is complex where the Cotton Valley is welded to basement and onlaps a giant Smackover-Haynesville tilt block near the southwest edge of line d8519 (Fig. 3C). The Knowles Limestone forms the top of the Cotton Valley and is a distinctive moderate- to high-amplitude reflector. A series of mounded to clinoform reflections within the Knowles defines the initial position of the Cretaceous reef trend along the southwest margin of the Viosca Knoll and Destin Dome areas (Fig. 3C).

Lower Cretaceous strata contain mainly siliciclastic rocks in the northeastern part of the salt basin and carbonate rocks in the southern and western parts (Fig. 2). Carbonate rocks include the reefal strata of the James and Andrew Formations, which have been the focus of exploration efforts in the Mobile and Viosca Knoll Areas (Petty, 1999; Montgomery et al., 2002). Lower Cretaceous strata are dominated by subparallel seismic reflections where siliciclastic strata pass into carbonates, and the reefal rocks are concentrated near the shelf break and include mounded and clinoform signatures. Thus, the subparallel reflections define a coastal plain and platform lagoon behind the shelf-margin reef trend (Montgomery et al., 2002). The Ferry Lake Anhydrite extends across the region (Petty, 1995) and forms a high-amplitude seismic marker that helps subdivide the Lower Cretaceous section (top Kl).

Pashin et al. 420 ▶

The base of the Tuscaloosa Group, which marks an unconformity between Lower and Upper Cretaceous strata (Mancini and Puckett, 2005), is not readily identified in seismic profiles. However, a prominent downlap surface defined by low-angle clinoforms (top Klu) corresponds with the contact between the sandstone of the Lower Tuscaloosa Group and the overlying Tuscaloosa marine shale. The gently dipping reflections in the Upper Cretaceous strata define a sediment wedge that pinches out at the shelf margin; they mark a major landward shift of coastal onlap and the development of a chalk-rich carbonate ramp atop the Lower Cretaceous platform. Paleocene through Oligocene strata are domi-

nated by shale and limestone and exhibit stratal geometry similar to the Upper Cretaceous section, and the top of the Tampa Limestone forms a strong reflector approximating the Oligocene-Miocene boundary. Middle and Upper Miocene strata of the Pensacola Clay constitute the bulk of the Miocene-Quaternary section, which extends to the seabed. Sandstone units in the Pensacola Clay form important targets for natural gas (Smith, 1991). The Miocene-Quaternary section thickens seaward to more than 6,500 feet, and the seismic expression includes subparallel to divergent reflections, clinoforms, and channel fills.

Structural Framework

Salt-tectonic structures in the De Soto Canyon salt basin exhibit a great variety of structural styles, and four distinct structural provinces were defined. These structural provinces include the (1) Destin fault system, (2) salt pillow province, (3) diapir province, and (4) salt roller province (Fig. 4). The Destin fault system is a peripheral fault system that formed near the updip limit of salt in the northeastern part of the basin in the Destin

Dome and Pensacola areas, and the salt pillow province formed just basinward of the fault system. The diapir province, by contrast, is in the structurally deepest part of the basin, which is in the southwestern Destin Dome area. The salt roller province is located in the western part of the basin, mainly in the Mobile, Viosca Knoll, and western Destin Dome areas.

Destin fault system

The Destin fault system forms an arcuate peripheral fault trend that is developed near the northeastern margin of the De Soto Canyon salt basin in the Destin Dome and Pensacola Areas (Figs. 3A, 3C, and 4). Pre-

vious workers mapped the fault system as a continuous, branching fault system (MacRae and Watkins, 1992, 1996), but new mapping indicates that the eastern part of the fault system comprises multiple normal faults

Pashin et al. 421 ▶

offset by relay ramps. The western part of the fault system strikes east-northeast and is composed of numerous down-to-basin normal faults that have traces shorter than 10 miles and are offset by relay ramps. Most of these faults are about 10 miles basinward of the northeast limit of salt and are arranged in an en echelon pattern that gives a dextral sense of shear. The eastern part of the fault system strikes northwest and contains faults having traces as long as 50 miles. Displacement of the eastern faults is mainly regional (down-to-basin), although some counterregional faults exist basinward of the longer regional faults (Figs. 3A, 3C). Vertical separation of the faults is consistent from the base of the Norphlet Formation to the top of the Smackover Formation and decreases upward in younger strata. The faults appear to terminate in the Upper Cretaceous section (Fig. 3A), and no faults could be mapped with consistency above the Ferry Lake Anhydrite.

Line d8537 traverses the two main faults in the eastern part of the fault system and reveals a pair of half

grabens, each having a hanging-wall rollover fold and a companion footwall uplift (Fig. 3A). This is the typical style of the fault system. The faults dip about 50° SW (Fig. 5A). Strata dip as steeply as 28° in the hanging wall block, and strata in the footwall uplifts locally dip steeper than 10°. Line d8519 (Fig. 3C) depicts combined regional and counterregional faulting. In this profile, the Destin fault system contains a regional fault and a counterregional fault that intersect the base of salt, and yet the overall geometry resembles the half grabens in Line d8537. In the interior of the structure, second-order synthetic and antithetic faults intersect the main faults. Seismic profiles reveal that virtually all hanging-wall rollover folds in the Destin fault system form a point or line weld with the top of basement regardless of salt thickness or fault length. Indeed, the thickness of the Louann Salt and the height of the footwall uplift are the primary determinants of the maximum displacement of the major faults.

Salt pillow province

Broad salt pillows that form the cores of large anticlines are a signature feature of the De Soto Canyon salt basin (MacRae and Watkins, 1992, 1993, 1995, 1996). The largest salt pillow forms the core of Destin Dome, which extends from the Pensacola area southeastward into the Destin Dome area (Figs. 3A, 4). Destin Dome is located a short distance basinward of the Destin fault system. The dome is a broad, open

structure and dip is generally less than 4°. Numerous small-displacement normal faults are developed in Cretaceous strata in the crestal region of the structure. Displacement appears to be greatest in the central parts of the crestal faults and diminishes toward the tips. Therefore, the crestal structures can be classified as dislocation faults (Gibbs, 1989). The southwest flank of the structure dips slightly steeper than the northeast

Pashin et al. 422 ▶

limb, and all stratigraphic markers are deformed save for the modern seabed (Figs. 3A, 5A). Stratigraphic thickness is fairly uniform across the dome in the Jurassic-Lower Cretaceous section (Js-Klu), whereas significant thinning over the crest is readily apparent in the Upper Cretaceous-Miocene section (Sputum).

A series of small salt pillows occur in the east-central Destin Dome area basinward of the giant Destin Dome pillow (Figs. 3A, 3B). Strata above these pillows form four-way structural closures, although the crestal regions are breached by normal faults. Some pillows are connected to the main Destin dome salt pillow, whereas others are isolated by salt welds. For example, the smaller salt pillow in Line d8537 (Fig. 3A) is attached to the Destin Dome pillow on the northeast and is bounded by a horizontal salt weld on the southwest. Strata dip steeper than 9° at the top of the Smackover Formation, whereas no anticline is apparent at the top of the Ferry Lake Anhydrite (top Kl). How-

ever, crestal faults do offset the Ferry Lake, indicating some late-stage extension. Regionally, only two of the smaller pillow related anticlines involve strata above the Ferry Lake Anhydrite (Fig. 6).

Line d8543 is a transect through a unique salt pillow (Fig. 3B). The pillow has a nearly flat bottom and has an asymmetrical profile that verges northeast. A small graben is developed southwest of the crest of the structure in the lower part of the Smackover Formation, and small normal growth faults having regional dip are developed on the flanks. In the northeast limb of the anticline, the Smackover Formation is connected to the basement surface in a series of fault-tip welds that are interpreted to be separated by a pair of localized salt rollers. The southwestern margin of the anticline is defined by an extensive salt weld. No deformation is apparent above the Haynesville Formation, and the salt-cored anticline is truncated at the base of the Cotton Valley Group by a pronounced angular unconformity.

Diapir province

Salt diapirs are numerous in the deepest part of the De Soto Canyon salt basin (Figs. 3A, 4B). A large, isolated diapir is located in the Viosca Knoll (North) area, and some small, poorly imaged diapirs occur in the western Mobile area. The upper parts of the diapirs are well imaged, whereas imaging of the flanks and bases of the structures is relatively poor. Most diapirs appear to be rooted on basement, and remnant salt masses are isolated by horizontal salt welds. Some dia-

pirs appear as detached masses, although it is inconclusive whether the seismic profiles record overhangs of diapirs having central salt stocks or record detached masses separated from the parent salt by vertical welds. Nearly all of the diapirs pierce Upper Cretaceous strata, and most terminate in the Tertiary section.

Normal faults and rim synclines are common near the base of the diapirs, and some turtle structures

Pashin et al. 423 ▶

are imaged where flanking strata are grounded on basement (Fig. 3A). Most seismic reflections are steep adjacent to the diapirs or vertical welds and flatten away from the main salt stocks. Outcrop investigation of Mexican diapirs in the Coahuila fold belt indicate that flanking beds can be nearly vertical, tangentially abutting the margins of diapirs, and thus dip too steeply to be imaged in conventional seismic reflection profiles (Giles and Lawton, 2002). The structural expression of

the tops of the diapirs is variable. In line d8537, for example, a crestal graben system is developed above one diapir, whereas strata are apparently deformed into a drape anticline above a strong caprock reflection at the top of the southwestern diapir. These structures indicate that passive diapirism gave way to active diapirism as salt movement waned and overburden began to accumulate. None of the diapirs appear to pierce the top of the Oligocene section.

Salt roller province

Salt rollers dominate the structural framework in the western part of the salt basin (Fig. 3C). The salt rollers are typically bounded by regional-dipping normal faults that have a planar to listric geometry. The faults separate a series of half grabens containing rollover folds, roho structures, and tilt blocks that are developed primarily in Jurassic strata. All normal faults associated with the salt rollers have maximum displacement at the top of the Louann Salt, and heave exceeds 6 miles in the southwestern part of the Viosca Knoll area, where a large Smackover-Haynesville block has been rafted basinward (Figs. 4A, 7A). The vast majority of the extensional faults are restricted to the Smackover-Cotton Valley section. However, some faults offset the Knowles Limestone, particularly in the updip reaches of the Mobile and Viosca Knoll areas. Although regional faulting is dominant, localized arrays of counterregional faults are developed (Fig. 7A).

Structural contour maps and and 3-D visualizations of the base of the Smackover reveal an array of arcuate normal faults that extend from the Mobile and Viosca Knoll areas into the western Destin Dome area (Figs. 4A, 7A). The faults strike effectively east-west in the Mobile area and turn to a northwest strike in the Destin Dome area. In general, the throw of the faults increases southwestward down regional dip and southeastward along strike (Figs. 3A, 4A). The geometry of faults having large trace lengths changes as displacement increases toward the southeast (Fig. 7B). Near the northwestern ends of the faults, the faults tend to have a planar geometry. As displacement increases, the faults become listric and can be traced into horizontal salt welds in the diapir province, which forms the heart of the salt basin. The updip margin of the salt roller province connects with the peripheral faults of the Destin fault system in the northwestern Destin Dome area (Fig. 4A).

Pashin et al. 424 ▶

Seismic line d8519 is a long transect showing the geometry of salt rollers southwest of the Destin fault system to the Cretaceous shelf margin (Fig. 3C). Near the northeast end of the salt roller province, faults are dominantly planar, and some of the faults form line or point welds with the basement surface. In this area, the structural style is dominated by half grabens in which faults lose displacement upward, terminating in the Haynesville section.

In the southwestern part of the seismic line, two large salt rollers are associated with a large roho structure that contains the thickest Smackover-Haynesville section in the salt basin. Roho structures are half gra-

bens having listric faults that sole out into horizontal salt welds. The welds below rohos have strong fault reflections attributed to remnant salt along the basal detachment (Rowan *et al.*, 1999). Near the Cretaceous shelf margin, immediately southwest of the roho, a large, steeply dipping tilt block is imaged. The tilt block appears to contain bed-parallel slip planes, including one bounding a slump block, and the block is locally welded like basement in a style resembling a stack of dominoes. Basinward of the tilt block the Cotton Valley sediment wedge is welded to basement, and Smack-over-Haynesville strata are absent.

Structural Evolution

The salt-tectonic evolution of the De Soto Canyon salt basin is highly complex, with each class of salt structure having a distinctive structural chronology (Fig. 8). Restoration of line d8537 reveals structural relationships among the peripheral faults and broad salt pillows (Fig. 5A). Restoring of the top of the Smack-over-Haynesville section shows that it pre-dates structural growth. Flattening of the Knowles limestone marker indicates that the peripheral faults and associated rollover folds and footwall uplifts began growing during Cotton Valley deposition, as did an embryo of the small salt pillow south of Destin Dome. Total extensional strain during this time was only 0.8% in the restored part of the cross section.

Growth of the southwestern salt pillow and the southwestern fault of the Destin fault system was effectively complete shortly after deposition of the Ferry Lake Anhydrite; the northeastern fault was active until Paleocene time. Decreasing displacement up the fault planes suggest that growth rate decelerated, and termination of fault growth corresponds with welding of the hanging-wall blocks to basement. Growth of Destin Dome is not obvious in the restorations until Late Cretaceous-Oligocene interval. Thus the dome largely post-dates the Destin Fault System. Although many of the individual structures along this transect have significant vertical separation and amplitude, total extensional strain is only 1.4%, and most deformation

Pashin et al. 425 l

can be attributed to salt withdrawal during regional subsidence.

Models of total effective subsidence document diachronous salt pillow development in the Destin Dome and Pensacola areas (Figs. 6, 9). Early Cretasubsidence during Hosston-Ferry ceous deposition indicates major salt withdrawal in the diapir province and accumulation of salt in an arcuate ridge composed of elongate salt pillows (Fig. 9A). The Mooringsport-Lower Tuscaloosa model shows continued salt withdrawal within the diapir province and restriction of pillow growth to the northwestern part of the arcuate ridge in a structure herein called ancestral Destin Dome (Fig. 9B). These models confirm that the classic Destin Dome structure did not grow significantly until Tuscaloosa-Midway deposition. The Tuscaloosa-Midway model, moreover, indicates reduction of the rate of salt withdrawal in the diapir province coupled with significant withdrawal in ancestral Destin Dome (Fig. 9C). The Wilcox-Tampa realization indicates a major episode of growth in Destin Dome, significant subsidence in and around the structure, and greatly reduced subsidence in the diapir province (Fig. 9D). Miocene and younger growth, by contrast, is restricted to the crestal region of the dome. Mapping structural traces and culminations indicates development of multiple four-way closures during Hosston-Ferry Lake deposition (Fig. 6). Loci of pillow formation has migrated northward and eastward through time, with formation of ancestral Dome between Hosston and Lower Tuscaloosa deposition. The northwestern part of Destin Dome overlaps the ancestral structure, and the axial trace of the pillow complex continues to migrate northeast through Miocene time.

The salt diapirs of the De Soto Canyon salt basin arguably had the longest span of formation of any structures in the salt basin (Fig. 8). The normal faults and rim synclines near the bases of the diapirs (Fig. 3A) suggest an initial phase of reactive diapirism (Vendeville and Jackson, 1992a, b). However, flattening of seismic reflections away from the margins of the diapirs is suggestive of prolonged downbuilding and passive growth (e.g., Rowan, 1995; Giles and Lawton, 2002; Fig. 8). Indeed, the lack of overburden above passive diapirs can provide outlets for salt by dissolution and probably contributed significantly to deflation of the parent Louann salt mass.

Active diapirism and turtle formation in the De Soto Canyon salt basin apparently began during the Late Cretaceous as the flanking strata began grounding on basement, thereby cutting off salt supply. As the salt supply was exhausted, sedimentation rate exceeded piercement rate, thereby burying the diapirs. Caprock reflections may mark dissolution of salt and mineralization prior to burial, and crestal grabens appear to have formed in response to differential compaction of sediment around the diapirs as downbuilding ceased, perhaps coupled with late-stage movement of buoyant salt.

Pashin et al. 426 ▶

Whereas most classes of structures in the salt basin evolved through large spans of geologic time, the salt rollers and associated folds and faults were largely Jurassic structures and only a few of the faults extended into Lower Cretaceous strata. Early formation of the rollers was readily apparent in the restoration of line d8519 (Fig. 5B). Restorations of the base of the Smackover Formation and the top of the Smackover-Haynesville interval established an extensional strain of 52 percent during the Late Jurassic (Fig. 5B), and diverging reflections within the rollover structures indicated that extensional faulting was initiated at the start of or during Smackover deposition (Fig. 3C).

. The rapid formation of the rollers and related structures, coupled with broadly arcuate nature of the fault systems (Fig. 7) indicates formation of a giant car-

bonate bank during a major episode of gravitational shelf spreading. Association of diapirs with rollerrelated decollements (Fig. 7B), moreover, suggests that gravitational spreading played a role in reactive diapirism. Flattening the top of the Knowles Limestone and younger markers indicates that post-Haynesville deformation is restricted mainly to folding in response to late-stage salt withdrawal, which was pronounced during the Early Cretaceous (Fig. 5B). The giant tilt block near the southwest end of line d8519 (Fig. 3C) indicates that a significant volume of Smackover-Haynesville sediment was rafted basinward, and rafted Jurassic fault blocks have been imaged not only at the edge of the Viosca Knoll Area (Figs. 4A, 5A), but in deep water south of the MAFLA shelf (Pilcher et al., 2012).

Burial and Thermal History

Burial history curves from two wells, one from the crestal region of Destin Dome and the other in the salt roller province of the Viosca Knoll Area can be considered as end-member curves for the De Soto Canyon salt basin (Fig. 10). The wells show a general decrease in the rate of total effective subsidence through time (Fig. 10), which is typical of passive shelf-margin successions (Xie and Heller, 2009). Subsidence rate is highest during Norphlet-Cotton Valley deposition, although a significant decrease of subsidence rate corresponds with Knowles Limestone deposition and the transition to carbonate platform sedi-

mentation. Subsidence rate decelerated during the Late Cretaceous, particularly near the crest of Destin Dome, reflecting late-stage inflation of the salt pillow (Fig. 9). Subsidence rate increased markedly during the Miocene, reflecting a major influx of sediment across much of the MAFLA shelf (Fig. 10B). Burial history models suggest that subsidence rate decreased substantially around 9 Ma and that regional subsidence of the salt basin continues today. Isostatic calculations indicate that tectonic subsidence accounts for less than 40% of the total effective subsidence in the burial history models. Therefore, subsidence associated with sediment

Pashin et al. 427 ▶

loading, salt withdrawal, and compaction accounts for the majority of the accommodation space in the basin.

Wellbore temperature data from the De Soto Cansalt basin demonstrate that bottom-hole von temperature can exceed 225°C at depths greater than 23,000 feet. Geothermal gradient is only 5.8°C/1,000 feet from near the surface to about 13,000 feet and increases to 9.9°C/1,000 feet at greater depth, indicating a decrease in thermal conductivity at depth that does not correspond with any tangible lithologic change. The geothermal gradient maintains a high degree of consistency across the salt basin (Nagihara and Jones, 2005; Nagihara and Smith, 2005). Ancient temperature profiles in the De Soto Canyon salt basin almost certainly have followed a classic post-rift thermal decay; however, the magnitude of this decay is poorly constrained.

Lopatin modeling indicates that present-day thermal maturity levels are quite high in the De Soto Canyon salt basin; in all wells studied, the Smackover Formation sits in or beyond the main gas generation window (Fig. 10). Interestingly, the aforementioned decrease in geothermal gradient with depth corresponds with calculated maturity levels of $R_{\rm o} \sim 1.0$, which are in

the thermogenic gas window. Accordingly, this decrease may be a product of geopressure related to free gas in the system. Modeling of vitrinite reflectance indicates that the rate of maturation was fairly constant during the first 65 million years of burial (Fig. 10C). Maturation rate decreased significantly during the Late Cretaceous, and this change corresponds with a decrease of subsidence rate throughout the salt basin. Increased burial rate from 32 to 9 Ma, however, has apparently had only a minor effect on thermal maturity.

Modeling of wells in the De Soto Canyon salt basin indicates a relatively short history of oil expulsion in the Smackover Formation; most expulsion occurs regionally between 130 and 90 Ma (Fig. 10D). The principal variables contributing to this short expulsion episode are rapid burial and thermal maturation during the Jurassic and Early Cretaceous. Of the wells modeled, expulsion is latest and most long-lived in Destin Dome Block 160, where the Smackover had reached a depth of less than 16,000 feet at 90 Ma (Fig. 10B). Expulsion is earliest and most rapid in Viosca Knoll Block 117, where the Smackover reached a burial depth of about 19,000 feet by that time (Fig. 10A).

Petroleum Systems Analysis

The essential elements of a petroleum system are source rock, reservoir rock, sealing strata, and overburden; essential processes include generation, expulsion, migration, trap formation, accumulation, and contain-

ment of petroleum (e.g., Magoon and Dow, 1994). The middle Smackover Formation has long been thought to be the principal source rock for hydrocarbons in salt basins of the MAFLA region because of TOC content

Pashin et al. 428 ▶

(0.25-1.75%), kerogen composition, and hydrocarbon geochemistry (*e.g.*, Sassen and Moore, 1988; Claypool and Mancini, 1989; Figs. 11 to 13).

Limited well control makes the distribution of candidate Smackover-Haynesville source rocks uncertain in the De Soto Canyon salt basin. Significant source-rock potential may exist in salt roller province, but little is known about the relationship between facies distribution and fault growth. One possibility is that structural highs above salt rollers were sites of shoaling, whereas offshore facies containing organic-rich source rocks, accumulated adjacent to the faults, which potentially formed important trans-stratal migration pathways (Fig. 11).

Aside from the Smackover Formation, Mesozoic strata in the De Soto Canyon salt basin are notably organic-lean, although some minor source rock intervals may be developed in the Jurassic-Cretaceous section (Petty, 1999). A prominent exception is the Tuscaloosa marine shale, which commonly has TOC content > 5% in southwest Alabama (Carroll, 1999). The marine shale is undermature in most regions, although the shale is projected to be within the oil window in the Viosca Knoll area (Fig. 10B) and may have higher thermal maturity in the deepest parts of the salt basin, such as the diapir province. Hence, a Tuscaloosa-sourced petroleum system may have been effective only in the diapir province and the deepest reaches of the Viosca Knoll shelf.

Productive Jurassic reservoirs in the section of the De Soto Canyon salt basin are primarily Norphlet gas reservoirs (Fig. 12). Chemical analyses from Alabama state waters establish that C₁ hydrocarbons compose 74 to 91 percent of the gas, and the dryness index averages only 92. Considering the elevated thermal maturity of the Norphlet-Smackover section (Fig. 10) this wetness indicates affinity with an oilprone source rock. The principal impurities in the gas are N2, CO2, and H2S. Hydrogen sulfide content averages 2% and can be >10%; it is thought to be the product of thermochemical sulfate reduction associated with the Pine Hill Anhydrite, which is at the top of the Louann Salt (e.g., McBride et al., 1987; Kugler and Mink, 1999). Multiple lines of evidence, including pyrobitumen and a fossil oil-water contact, point toward emplacement of Norphlet hydrocarbons as oil that was cracked to natural gas (Kugler and Mink, 1999).

Petroleum exploration has met with limited success in reefal deposits along the Lower Cretaceous shelf margin in the James and Andrew Formations, and sulfidic gas in these formations is thought to indicate affinity with Smackover source rocks (Petty, 1999; Nagihara and Smith, 2005). Importantly, much of the hydrocarbon potential of the De Soto Canyon salt basin remains untested, and so a substantial portfolio of undiscovered reservoirs may exist along the Lower Cretaceous shelf margin, above salt pillows, and in the diapir province.

Evaporite, shale, and carbonate units are common sealing strata. The Louann Salt and the Pine Hill Anhydrite form a prominent bottom seal that extends throughout the salt basins. Where these units are absent, the Norphlet-Cotton Valley section laps onto igneous and metamorphic basement rocks, which are typically impermeable and thus also have sealing capacity. Source rocks commonly double as reservoir seals (Sutton *et al.*, 2004), and offshore production from the Norphlet Formation indicates that lower and middle Smackover micrite can form reservoir seals. In the Mobile Area, pyritization along the Norphlet-Smackover contact during thermochemical sulfate reduction probably contributes to seal integrity.

The apparent lack of major Haynesville evaporites in the De Soto Canyon Salt Basin raises questions about the presence of sealing strata above the Smackover. Seals may be associated with the angular unconformity between the Smackover and Haynesville in the salt roller province, as well as a shale unit that forms the top of the Haynesville (Fig. 12). Shale units intercalated with with James and Andrew reefal reservoirs also appear to be reservoir seals (Petty, 1999). Upper Cretaceous shale and chalk form major reservoir seals in the Mississippi interior salt basin that traps hydrocarbon accumulations in Cretaceous sandstone (Pashin et al., 2000), but exploration efforts in Lower Tuscaloosa sandstone in the De Soto Canyon salt basin have yet to bear fruit (Petty, 1997). However, the Tuscaloosa may be an important CO₂ storage objective, as

is the case onshore (Koperna et al., 2009; Hovorka et al., 2013).

A range of stratigraphic, structural, and combination traps are known in the De Soto Canyon salt basin (Fig. 13), and numerous prospects remain to be tested. Norphlet reservoirs commonly form combination and stratigraphic traps. In the Mobile area, for example, elongate, biconvex eolian sandstone bodies arch over salt rollers, thereby trapping hydrocarbons where drape folds intersect the crests of the rollers (Story, 1998). Smackover potential is untested where unconformity traps may exist in the salt roller province, and migration of hydrocarbons up faults may have been an important process that facilitated reservoir charge (Fig. 12).

Reefal reservoirs in the James and Andrew formations can be classified as stratigraphic traps (Petty, 1999), and large parts of the reef tract remain untested. Additional combination traps may be associated with updip pinchout of Tuscaloosa Group sandstone on the flanks of Destin Dome (Petty, 1997). Seismic profiles and structure maps indicate that numerous structural trap types, including fault closures, rollover folds, pillow-cored anticlines, and diapir-related traps may be present. Three-way footwall closures are a dominant trap type in onshore Jurassic and Cretaceous reservoirs (Qi et al., 1998; Pashin et al, 2000), but similar structures have been disappointing in the Destin fault system, suggesting inadequate fault seals. Only one well has tested the small salt pillows southwest of Destin Dome, and that well was dry perhaps suggesting that

Pashin et al. 430 ▶

crestal faulting may pose seal risk. Only the flanking beds of the isolated diapir in the Viosca Knoll area have been tested, and none of the structures in the main diapir province have been drilled. Hence, potential traps exist in flanking beds, turtle structures, and in the crests of the diapirs.

Comparison of the timing of modeled Smackover oil expulsion with the depositional and structural chronology indicated that the Mesozoic stratigraphic traps, including Norphlet sandstone lenses and prospective Smackover-Haynesville unconformity traps, were in place before the end of expulsion (Fig. 13). The salt rollers and related structures were largely in place prior to petroleum expulsion, as were the reactive and passive segments of the salt diapirs. The small salt pillows

and ancestral Destin Dome also had formed prior to the end of modeled oil expulsion. Destin Dome and activephase diapirs, by contrast, formed largely after major expulsion.

Considering the low TOC content of the known Jurassic source rocks in the eastern Gulf of Mexico region, a strong possibility exists that generative potential was exhausted earlier than the modeled end of expulsion. For this reason, the critical moment is placed at the start of the Cretaceous near the midpoint of modeled oil expulsion, and structures that formed during or after the Late Cretaceous, after which most hydrocarbons would have moved through the petroleum system, are considered high risk.

Conclusions

Mesozoic strata in the De Soto Canyon salt basin record a complex structural evolution that had a strong impact on petroleum system development. Salt tectonic activity was initiated in the western part of the salt basin by a major episode of gravitational shelf spreading that included roller formation sediment rafting, and localized reactive diapirism. This event was instrumental in determining the stratigraphic and structural architecture of the Smackover-Haynesville carbonate bank. Passive diapirism occurred in the heart of the salt basin until the Late Cretaceous, giving way to active diapirism as salt supply began to be exhausted and sedimentation rate began to exceed the rate of piercement.

The Destin fault system formed near the periphery of the salt basin during Cotton Valley deposition, and significant fault movement ceased around the time that active diapirism began in the heart of the basin. Broad salt pillows began forming between the Destin fault system and the diapir province during Haynesville deposition. Pillow formation was highly diachronous; small pillows and the ancestral Destin Dome formed in the Early Cretaceous and the formation of the Destin Dome salt pillow began in the Late Cretaceous after major passive diapirism and peripheral faulting were complete.

Pashin et al. 431 ▶

The burial history of the basin was consistent with post-rift thermal decay and passive margin development. Sediment was accommodated by salt movement throughout the basin during the Late Jurassic and Early Cretaceous, and late-stage salt movement was concentrated in Destin Dome. Smackover carbonate entered the oil window during the Early Cretaceous, and modern maturity levels throughout the basin are well within the thermogenic gas window and are in places over mature. The marine shale of the Tuscaloosa Group was generally undermature, although these strata appeared to have recently entered the oil window in the deepest part of the basin.

Petroleum systems analysis indicates that the Smackover Formation contains the principal source rocks in the basin, and proven Mesozoic reservoirs are in Norphlet Sandstone, and to a lesser extent in Early Cretaceous reefal deposits near the shelf margin. Known and prospective reservoirs can generally be explained by short-range migration of petroleum, including migration along faults, particularly in the salt roller province. Sealing strata are thought to include carbonate and shale, although relationships are uncertain in many areas. Known hydrocarbon accumulations

are primarily combination and stratigraphic traps, and numerous prospective structures related to salt pillows and diapirs have yet to be tested. Results of petroleum systems analysis indicate that most structures in the basin formed prior to or during major hydrocarbon expulsion and thus are prospective. The salt basin is further being assessed for geologic CO₂ storage potential, and the same sandstone formations and reservoir seals that have been proven onshore also are present offshore, indicating significant potential for safe storage and CO₂ enhanced recovery operations.

The approach employed in this study reveals that the interrelationships between structure and sedimentation in Mesozoic salt basins are quite complex. Balancing, restoration, and computer visualization are important tools for diagnosing these complexities, which need to be understood to develop robust petroleum system models. The structural families observed in the De Soto Canyon salt basin are common in other Gulf of Mexico salt basins, and applying integrated structural and petroleum systems analysis can reveal genetic associations, as well as fundamental differences, that help inform exploration and resource development in a broad range of salt tectonic settings.

Acknowledgments

This research was supported by the U.S. Minerals Management Service (now BOEM) under various agreements and the U.S. Department of Energy (cooperative agreement DE-FE0026086) through the Southern States Energy Board (subgrant SSEB-SOSRA-981-OSU-2015-001rev). The manuscript was reviewed by Luke Walker and the Gulf of Mexico exploration team at Noble Energy, whose insight and suggestions substantially improved the quality of this contribution. This report was prepared as an account of work sponsored by an agency of the United States Government. Neither the United States Government nor any agency thereof, nor any of their employees, makes any

warranty, express or implied, or assumes any legal liability or responsibility for the accuracy, completeness, or usefulness of any information, apparatus, product, or process disclosed, or represents that its use would not infringe privately owned rights. Reference herein to any specific commercial product, process, or service by trade name, trademark, manufacturer, or otherwise does not necessarily constitute or imply its endorsement, recommendation, or favoring by the United States Government or any agency thereof. The views and opinions of authors expressed herein do not necessarily state or reflect those of the United States Government or any agency thereof.

References

- Angevine, C.L., P.L. Heller, and C. Paola, 1990, Quantitative sedimentary basin modeling: AAPG Continuing Education Course Notes Series 32, 256 p.
- Carroll, R.E., 1999, Burial and thermal maturation history of the Gilbertown area, southwest Alabama: GCAGS Transactions, v. 49, p. 162–171.
- Claypool, G.E., and E.A. Mancini, 1989, Geochemical relationships of petroleum in Mesozoic reservoirs to carbonate source rocks of Jurassic Smackover Formation, southwestern Alabama: AAPG Bulletin, v. 73, p. 904–924.
- Dobson, L.M., and R.T. Buffler, 1991, Basement rocks and structure, northeastern Gulf of Mexico: GCAGS Transactions, v. 41, p. 191–206.

- Dobson, L.M., and R.T. Buffler, 1997, Seismic stratigraphy and geologic history of Jurassic rocks, northeastern Gulf of Mexico: AAPG Bulletin, v. 81, p. 100–120.
- Gibbs, A.D., 1989, Structural styles in basin formation: AAPG Memoir 46, p. 81–93.
- Giles, K.A., and T.F. Lawton, 2002, Halokinetic sequence stratigraphy adjacent to the El Papalote diapir, north-eastern Mexico: AAPG Bulletin, v. 86, p. 823–840.
- Gradstein, F.M., J.G. Ogg, M. Schmitz, and G. Ogg., eds., 2012, The Geologic Time Scale 2012: Amsterdam, Elsevier, 1176 p.
- Groshong, R.H., Jr., 1994, Area balance, depth to detachment, and strain in extension: Tectonics, v. 13, p. 1488–1497.

Pashin et al. 433 ▶

- Groshong, R.H., Jr., J.C. Pashin, B. Chai, and R.D. Schneeflock, 2003, Predicting reservoir-scale faults with area balance: application to growth stratigraphy: Journal of Structural Geology, v. 25, p. 1645–1658.
- Hovorka, S.D., T.A. Meckel, and R.H. Treviño, 2013, Monitoring a large-volume injection at Cranfield, Mississippi—Project design and recommendations: International Journal of Greenhouse Gas Control, v. 18, p. 345–360.
- Hughes, D.J., 1968, Salt tectonics as related to several Smackover fields along the northeast rim of the Gulf of Mexico basin: GCAGS Transactions, v. 18, p. 320–330.
- Jackson, M.P.A., 1982, Fault tectonics of the East Texas Salt Basin: Texas Bureau of Economic Geology Circular 82–84, 31 p.
- Kopaska-Merkel., D.C., and J.W. Schmoker, 1994, Regional porosity evolution in the Smackover Formation of Alabama: Carbonates and Evaporites, v. 9, p. 58–75.
- Koperna, G., D. Riestenberg, R. Petrusak, and R. Esposito, 2009, Lessons learned while conducting drilling and CO₂ injection operations at the Victor J. Daniel Power Plant in Mississippi: Society of Petroleum Engineers paper SPE 124003, 26 p.
- Kugler, R.L., and R.M. Mink, 1999, Depositional and diagenetic history and petroleum geology of the Jurassic Norphlet Formation of the Alabama coastal waters area and adjacent Federal waters area: Marine Georesources and Geotechnology, v. 17, p. 215–232.
- MacRae, G., and J.S. Watkins, 1992, Evolution of the Destin Dome, offshore Florida, northeastern Gulf of Mexico: Marine and Petroleum Geology, v. 9, p. 501–509.

- MacRae, G., and J.S. Watkins, 1993, Basin architecture, salt tectonics, and Upper Jurassic structural styles, north-eastern Gulf of Mexico: AAPG Bulletin, v. 77, p. 1809–1824.
- MacRae, G., and J.S. Watkins, 1995, Early Mesozoic rift-stage half graben formation beneath the DeSoto Canyon salt basin: Journal of Geophysical Research, v. 100, p. 17795–17812.
- MacRae, G., and J.S. Watkins, 1996, DeSoto Canyon salt basin: Tectonic evolution and salts [sic] structural styles, *in* J.O. Jones, and R.L. Freed, eds., Structural framework of the northern Gulf of Mexico: GCAGS Special Publication, p. 53–61.
- Mancini, E.A., and T.M. Puckett, 2005, Jurassic and Cretaceous transgressive (T-R) cycles, northern Gulf of Mexico, USA: Stratigraphy, v. 2, p. 31–48.
- Mancini, E.A., R.M. Mink, B.L. Bearden, and R.P. Wilkerson, 1985, Norphlet Formation (Upper Jurassic) of southwestern and offshore Alabama: Environments of deposition and petroleum geology: AAPG Bulletin, v. 69, p. 881–898.
- Mancini, E.A., R.M. Mink, and B.L. Bearden, 1986, Integrated geological, geophysical, and geochemical interpretation of Upper Jurassic petroleum trends in the eastern Gulf of Mexico: GCAGS Transactions, v. 36, p. 219–227.
- Martin, R.G., 1978, Northern and eastern Gulf of Mexico continental margin stratigraphic and structural framework: AAPG Studies in Geology 7, p. 21–42.
- Magoon, L.B., and W.G. Dow., eds., 1994, The petroleum system—From source to trap: AAPG Memoir 60, 655 p.

- McBride, E.F., L.S. Land, and I.E. Mack, 1987, Diagenesis of eolian and fluvial feldspathic sandstones, Norphlet Formation, Rankin County, Mississippi, and Mobile County, Alabama: AAPG Bulletin, v. 71, p. 1019–1034.
- Montgomery, S.L., A.J. Petty, and P.J. Post, 2002, James Limestone, northeastern Gulf of Mexico: Refound opportunity in a Lower Cretaceous trend: AAPG Bulletin, v. 86, p. 381–397.
- Nagihara, S., and K.O. Jones, 2005, Geothermal heat flow in the northeastern Gulf of Mexico: AAPG Bulletin, v. 89, p. 821–831.
- Nagihara, S., and M.A. Smith, 2005, Geothermal gradient and temperature of hydrogen sulfide-bearing reservoirs, Alabama continental shelf: AAPG Bulletin, v. 89, p. 1451–1458.
- Pashin, J.C., R.H. Groshong, Jr., Jin and Guohain, 1998, Structural modeling of a fractured chalk reservoir: toward revitalizing Gilbertown Field, Choctaw County, Alabama: GCAGS Transactions, v. 48, p. 335–347.
- Pashin, J.C., D.E. Raymond, G.G. Alabi, R.H. Groshong, Jr., and Jin Guohai, 2000, Revitalizing Gilbertown oil field: Characterization of fractured chalk and glauconitic sandstone reservoirs in an extensional fault system: Alabama Geological Survey Bulletin 168, 81 p.
- Pearson, O.N., E.L. Rowan, and J.M. Miller, 2012, Modeling the Mesozoic-Cenozoic structural evolution of East Texas: GCAGS Journal, v. 1, p. 118–130.
- Petty, A.J., 1995, Ferry Lake, Rodessa, and Punta Gorda anhydrite bed correlation, Lower Cretaceous, offshore eastern Gulf of Mexico: GCAGS Transactions, v. 45, p. 487–493.

- Petty, A.J., 1997, Lower Tuscaloosa clastic facies distribution (Upper Cretaceous), Federal and State waters, eastern Gulf of Mexico: GCAGS Transactions, v. 47, p. 454–462.
- Petty, A.J., 1999, Petroleum exploration and stratigraphy of the Lower Cretaceous James Limestone (Aptian) and Andrew Formation (Albian): Main Pass, Viosca Knoll, and Mobile Areas, northeastern Gulf of Mexico: GCAGS Transactions, v. 49, p. 441–450.
- Pilcher, R.S., R.T. Murphy, and J. McDonough Ciosek, 2012, Jurassic raft tectonics in the northeastern Gulf of Mexico: Interpretation, v. 2, p. SM39–SM55.
- Pindell, J., and Kennan, L., 2001, Kinematic evolution of the Gulf of Mexico and Caribbean: GCSSEPM Foundation 21st Annual Bob F. Perkins Research Conference, p. 193–220.
- Qi Jiafu, J.C. Pashin, and R.H. Groshong, Jr., 1998, Structure and evolution of North Choctaw Ridge Field, Alabama, a salt-related footwall uplift along the peripheral fault system, Gulf Coast basin: GCAGS Transactions, v. 48, p. 349–359.
- Rowan, M.G., 1995, Structural styles and evolution of allochthonous salt, central Louisiana outer shelf and upper slope: AAPG Memoir 65, p. 199–228.
- Rowan, M.G., and R. Kligfield, 1989, Cross section balancing and restoration as an aid to seismic interpretation in extensional terranes: AAPG Bulletin, v. 73, p. 955–966.
- Rowan, M.G., M.P.A. Jackson, and B.D. Trudgill, 1999, Salt-related fault families and fault welds in the northern Gulf of Mexico: AAPG Bulletin, v. 83, p. 1454–1484.
- Sandwell, D.T., R.D. Müller, W.H.F. Smith, E. Garcia, and R. Francis, 2014, New global marine gravity model from

Pashin et al. 435 ▶

- CryoSat-2 and Jason-1 reveals buried tectonic structure: Science, v. 346, p. 65–67.
- Sassen, R., and C.H. Moore, 1988, Framework of hydrocarbon generation and destruction in eastern Smackover trend: AAPG Bulletin, v. 72, p. 649–663.
- Smith, C.C., 1991, Foraminiferal biostratigraphic framework, paleoenvironments, rates of sedimentation, and geologic history of the subsurface Miocene of southern Alabama and adjacent state and federal waters: Alabama Geological Survey Bulletin 138, 223 p.
- Story, C., 1998, Norphlet geology and 3-D geophysics of Fairway field, Mobile Bay, Alabama, *in* J.L. Allen and others, eds., 3-D seismic case histories from the Gulf Coast basin: Austin, Texas, GCAGS, p. 123–129.
- Sutton, S.J., F.G. Ethridge, W.R. Almon, W.C. Dawson, and K.K. Edwards, 2004, Textural and sequence-stratigraphic controls on sealing capacity of Lower and

- Upper Cretaceous shales, Denver Basin, Colorado: AAPG Bulletin, v. 88, p. 1185–1206.
- Vail, P.R., 1987, Seismic stratigraphy interpretation procedure: AAPG Studies in Geology 27, v. 1, p. 1–10.
- van Hinte, J.E., 1978, Geohistory analysis—Application of micropaleontology in exploration geology: AAPG Bulletin, v. 62, p. 201–222.
- Vendeville, B.C., and M.P.A. Jackson, 1992a, The rise of diapirs during thin-skinned extension: Marine and Petroleum Geology, v. 9, p. 331–353.
- Vendeville, B.C., and M.P.A. Jackson, 1992b, The fall of diapirs during thin-skinned extension: Marine and Petroleum Geology, v. 9, p. 354–371.
- Waples, D.W., 1980, Time and temperature in petroleum formation: AAPG Bulletin, v. 64, p. 916–926.
- Xie., X., and P.L. Heller, 2009, Plate tectonics and basin subsidence history: Geological Society America Bulletin, v. 121, p. 55–64.

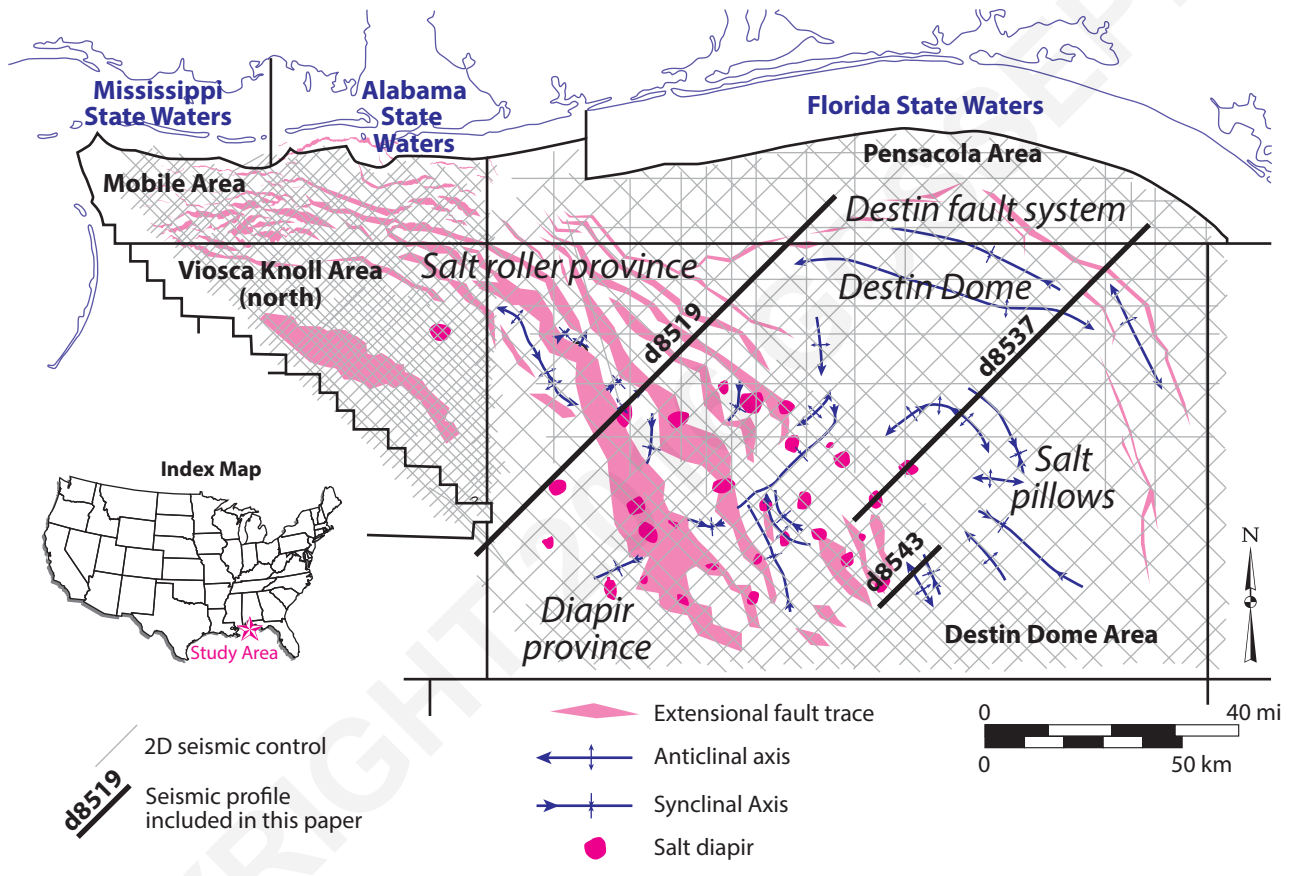


Figure 1. Map of study area showing major structural features and 2D seismic coverage used in this study.

Pashin et al. 437 ▶

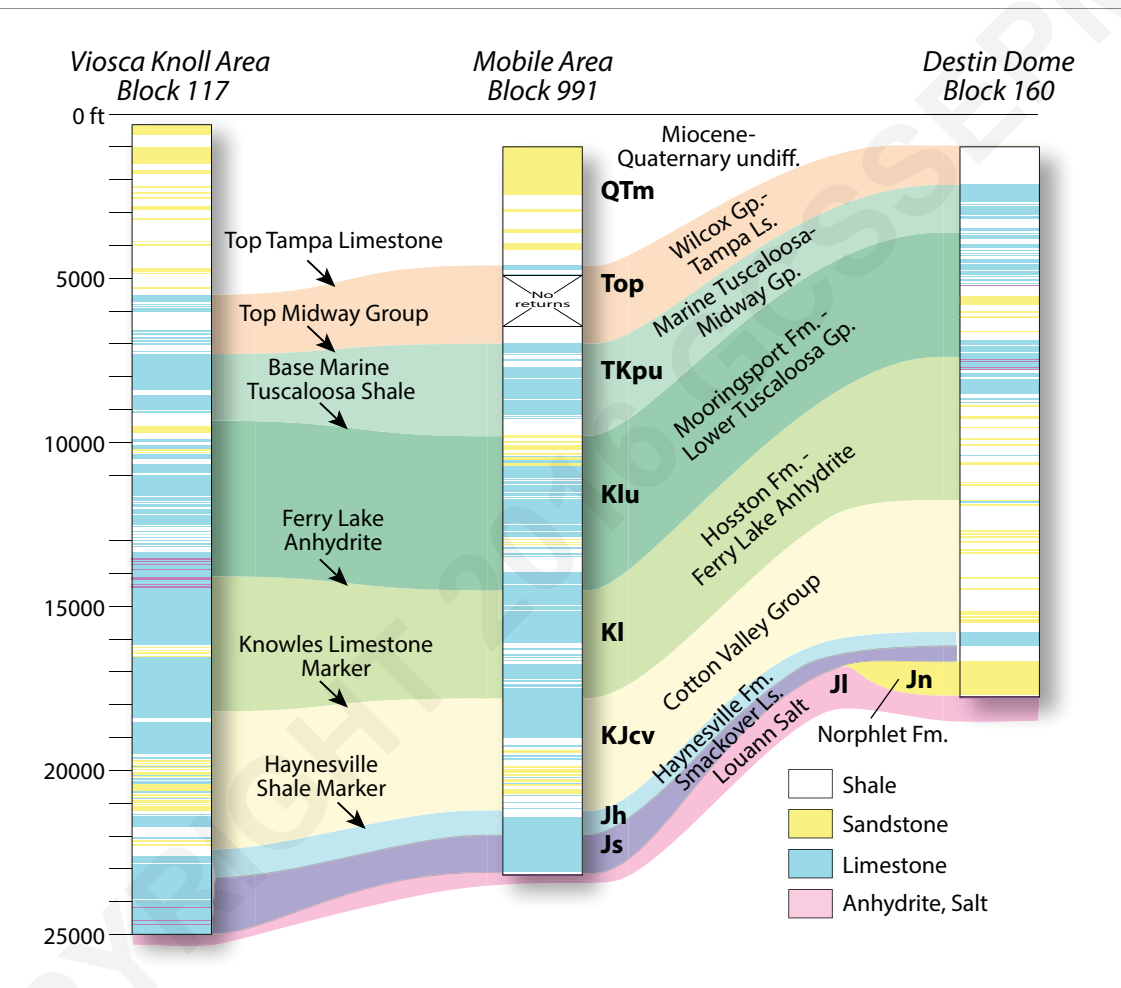


Figure 2. Lithologic columns of selected wells showing rock types and major stratigraphic intervals used in this study.

Pashin et al. 438 ▶

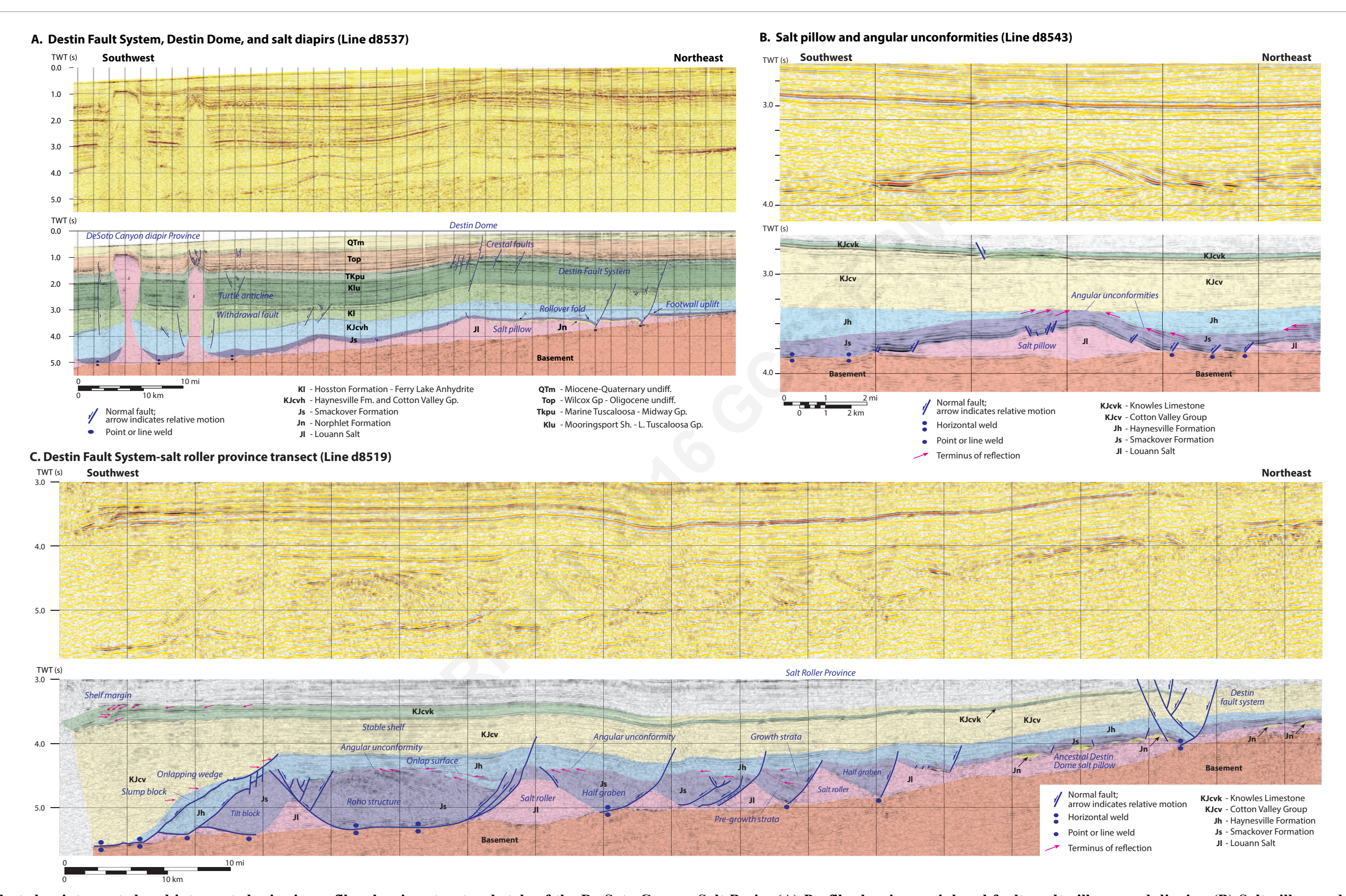
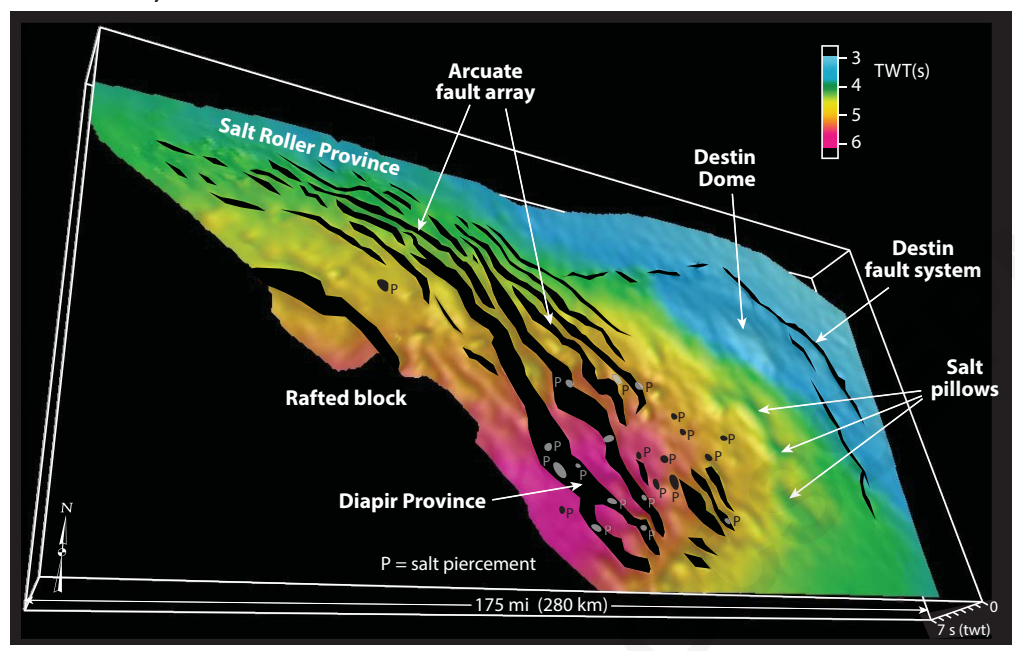


Figure 3. Selected uninterpreted and interpreted seismic profiles showing structural style of the De Soto Canyon Salt Basin. (A) Profile showing peripheral faults, salt pillows, and diapirs. (B) Salt pillow and angular unconformities constraining Jurassic growth. (C) Seismic transect from the Destin Fault System through the salt roller province.

Pashin *et al.* 439 ▶

A. 3D model, Smackover structure



B. 3D model, Ferry Lake structure

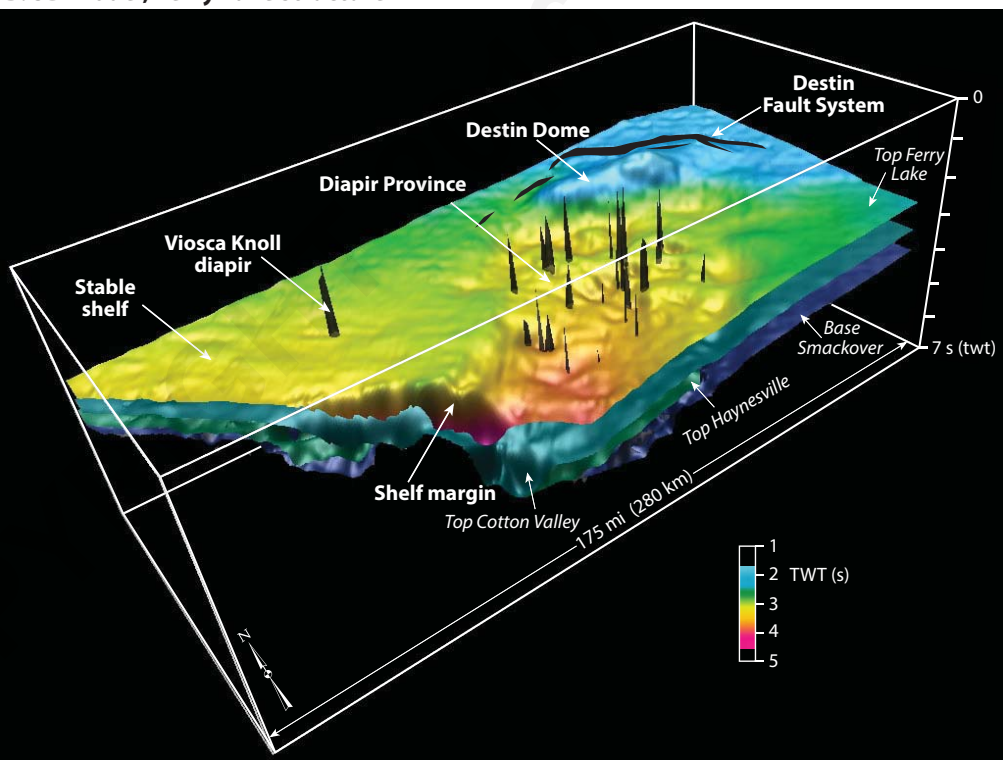


Figure 4. 3D visualizations of geologic structure in the De Soto Canyon Salt Basin. (A) Model of top of Smackover Formation showing relationships among major faults, folds, and salt piercements. (B) Model of the top of the Ferry Lake Anhydrite showing locations of mappable faults, folds, and salt diapirs.

Pashin *et al.* 440 ▶

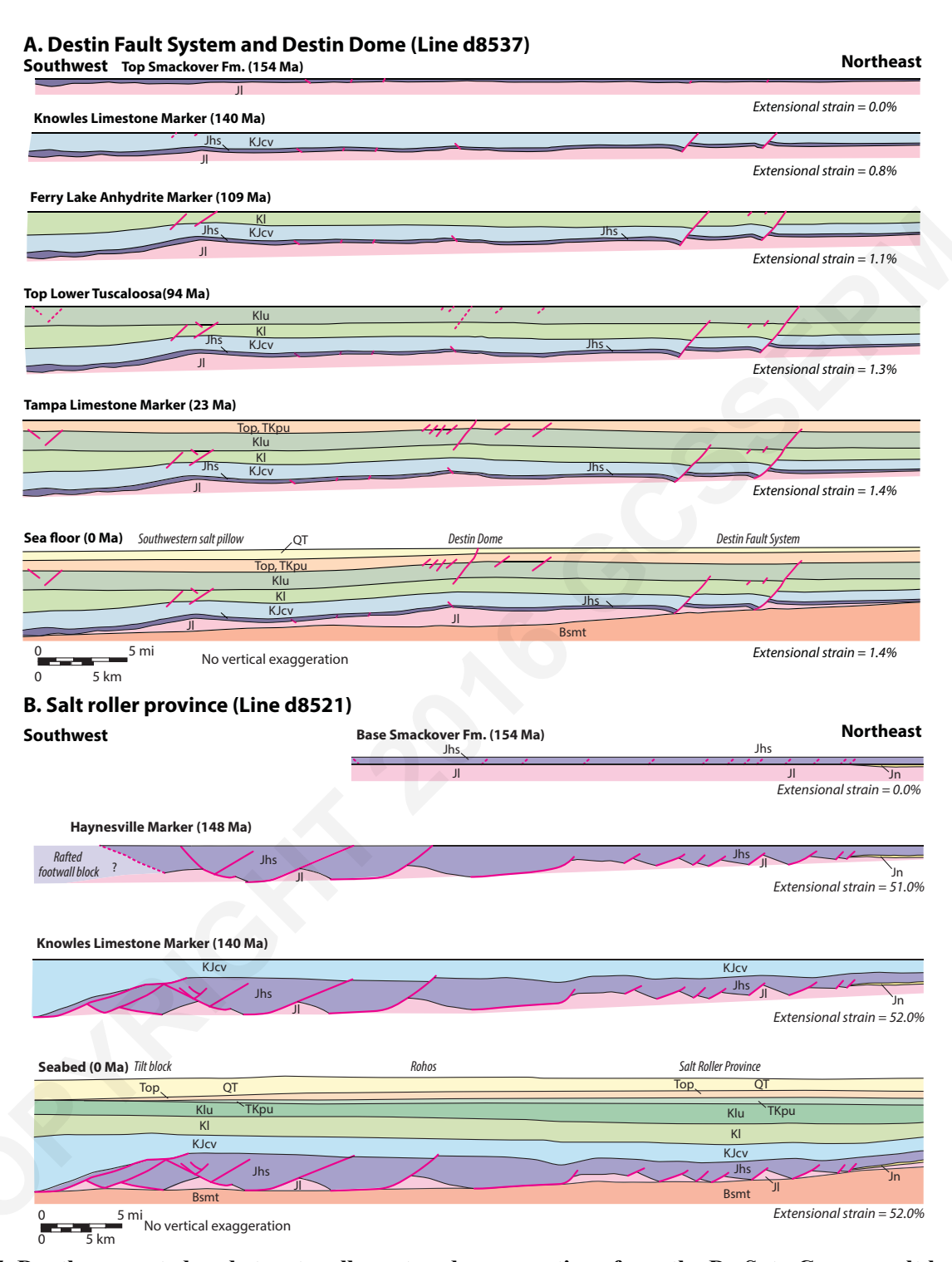


Figure 5. Depth converted and structurally restored cross sections from the De Soto Canyon salt basin. (A) Sequential restoration showing evolution of the Destin fault system, Destin Dome, and associated salt pillows. (B) Sequential restoration showing early formation of roller province and subsequent development of a stable continental shelf.

Pashin et al. 441 ▶

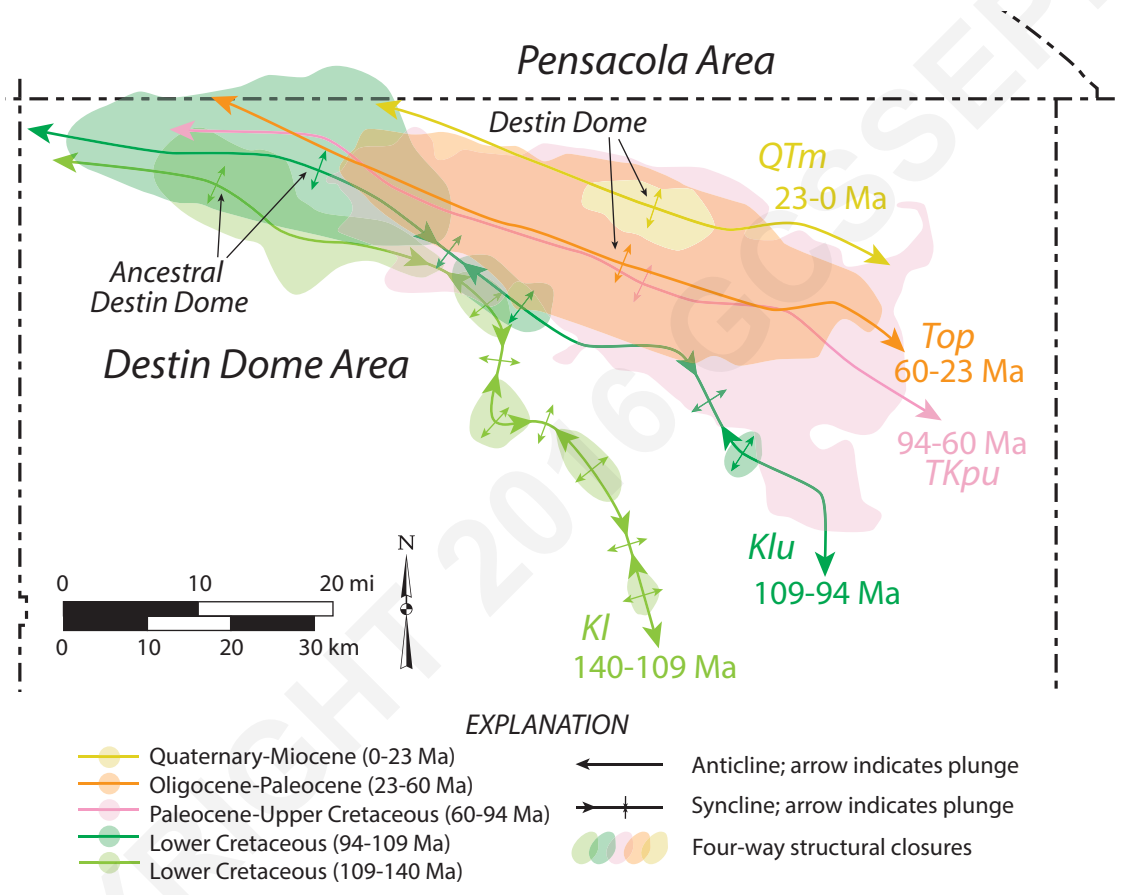
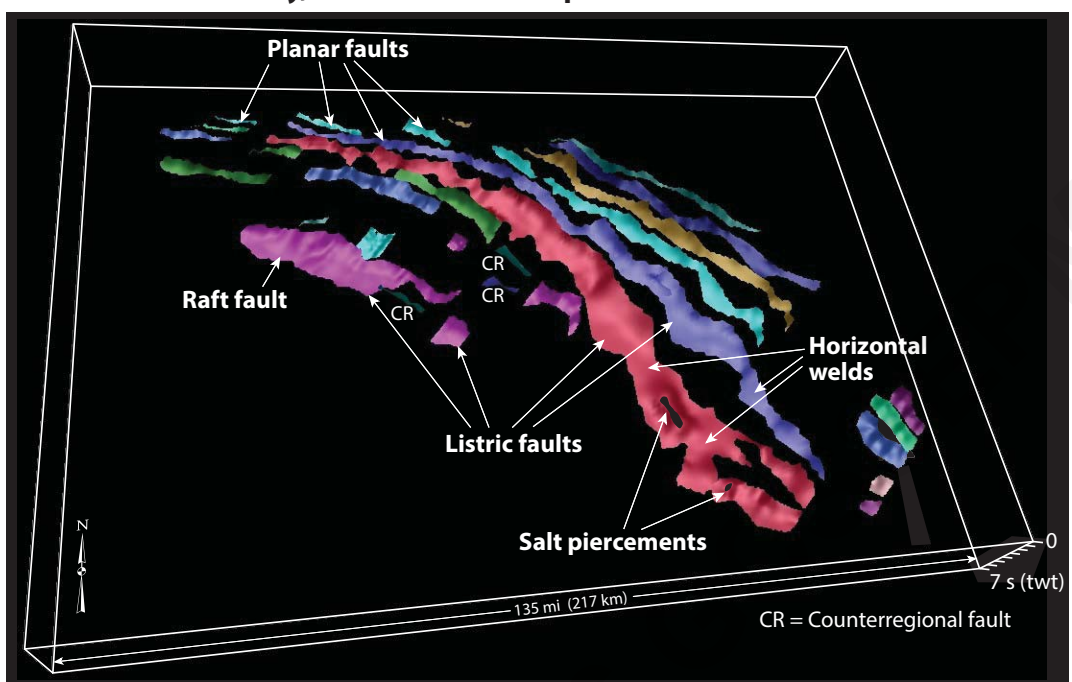


Figure 6. Structural trace maps showing locations structural closures through time and diachronous evolution of broad salt pillows in the De Soto Canyon salt basin.

A. Arcuate Fault Array, Salt Roller and Diapir Provinces



B. Lateral Changes Along Arcuate Fault

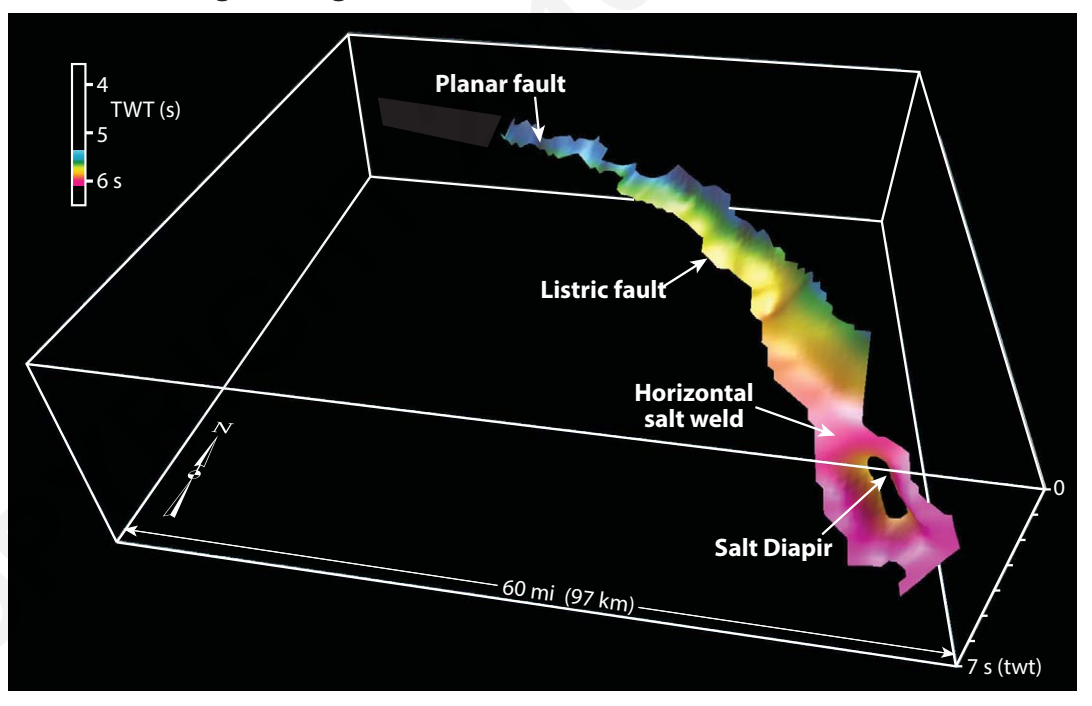


Figure 7. 3D realizations of fault networks in the salt roller province. (A) Arcuate fault array interpreted to developed by gravitational spreading of the Smackover-Haynesville carbonate bank. (B) Model of along-strike changes in fault geometry showing transition from planar fault to listric fault, to horizontal weld (decollement) below salt diapir. Association of diapirs with decollements suggests relationship between gravitational shelf spreading and initial stage of reactive diapirism.

Pashin et al. 443 ▶

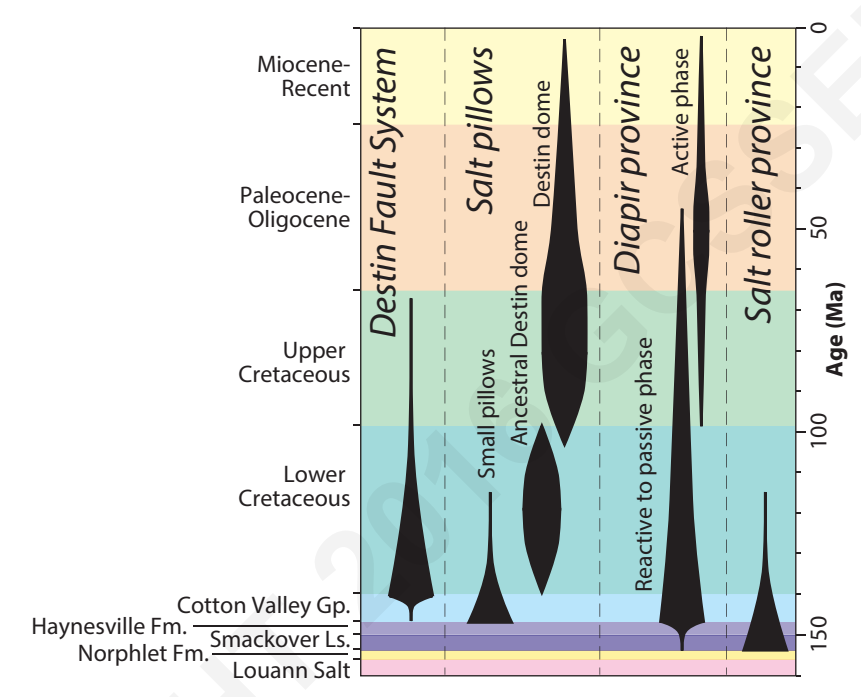


Figure 8. Structural chronology of the De Soto Canyon salt basin.

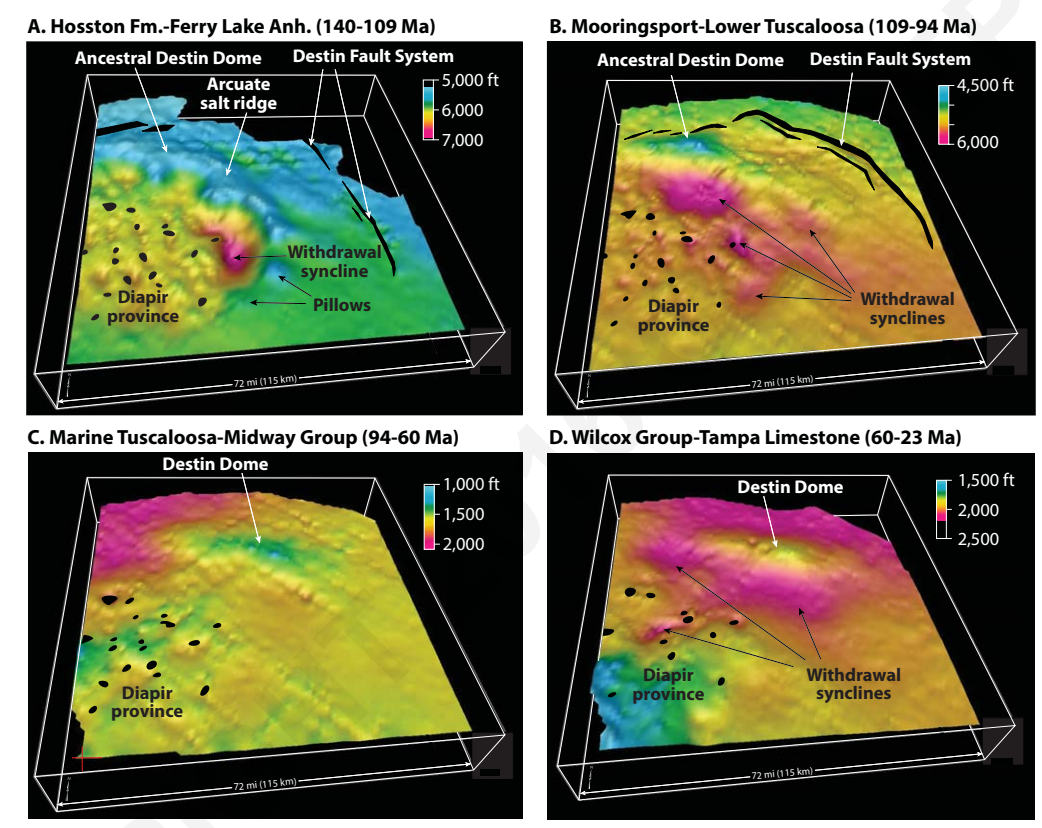


Figure 9. 3D models of total effective subsidence demonstrating diachronous evolution of large salt pillows and major formation of Destin Dome after formation of the Destin fault system. (A) Arcuate array of salt pillows along margin of diapir province. (B) Formation of ancestral Destin Dome. (C) Initial formation of Destin Dome concomitant with deflation of the ancestral structure in the northwest. Late-stage formation of Destin Dome by withdrawal of salt along the flanks of the structure.

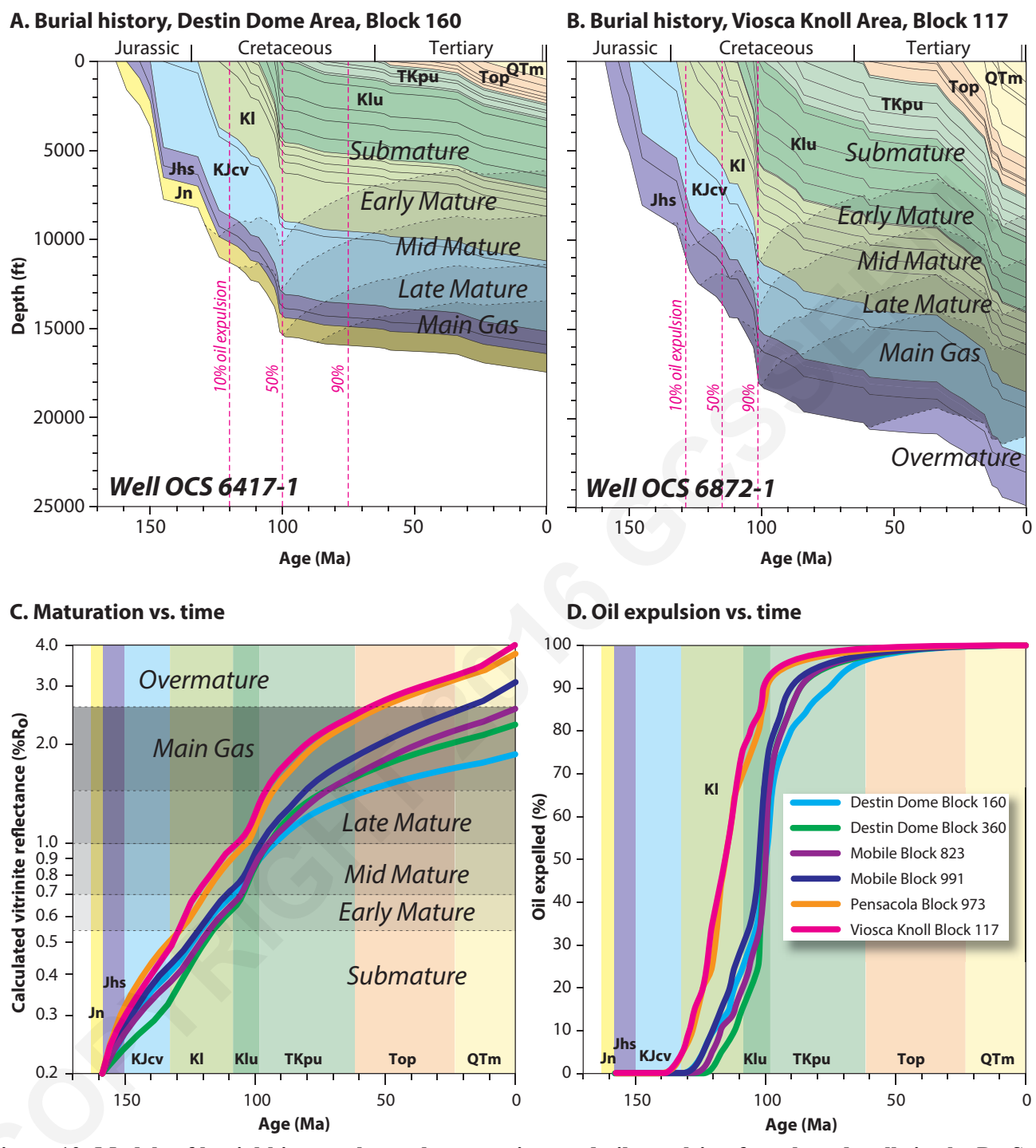


Figure 10. Models of burial history, thermal maturation, and oil expulsion for selected wells in the De Soto Canyon salt basin. (A) Burial history model for well near crest of Destin Dome. (B) Burial history model for well in salt roller province. (C) Plots of thermal maturation vs. time for selected wells. (D) Plots of Smack-over oil expulsion vs. time for selected wells.

Pashin et al. 446 ▶

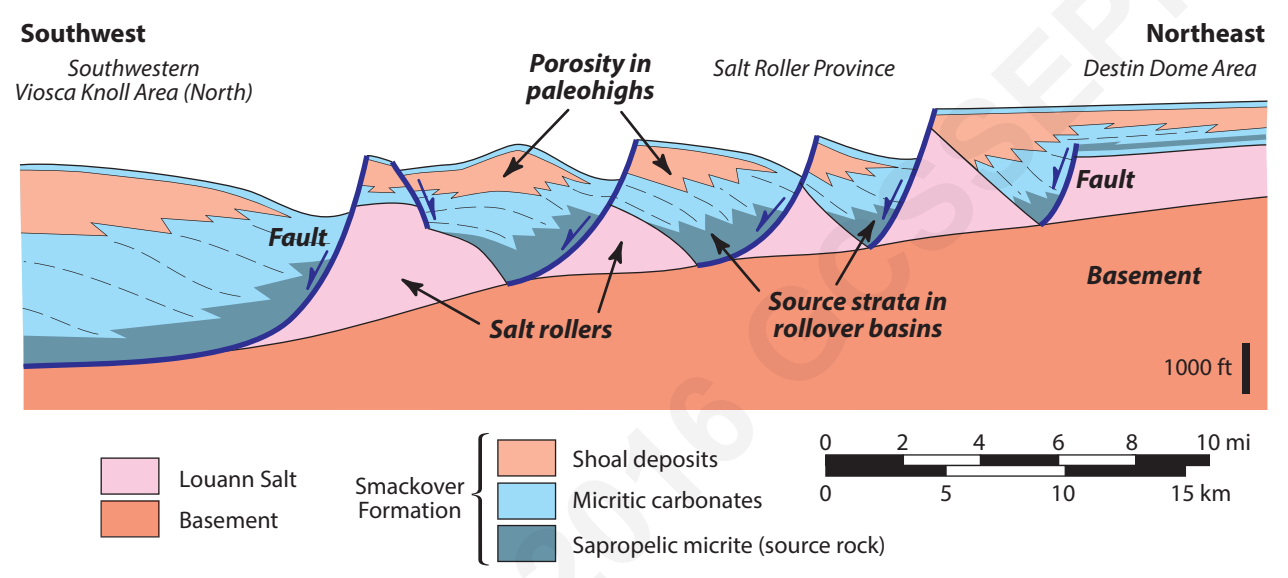


Figure 11. Schematic diagram showing interpretation of possible Smackover source rock and reservoir facies in salt roller province.

Pashin et al. 447 ▶

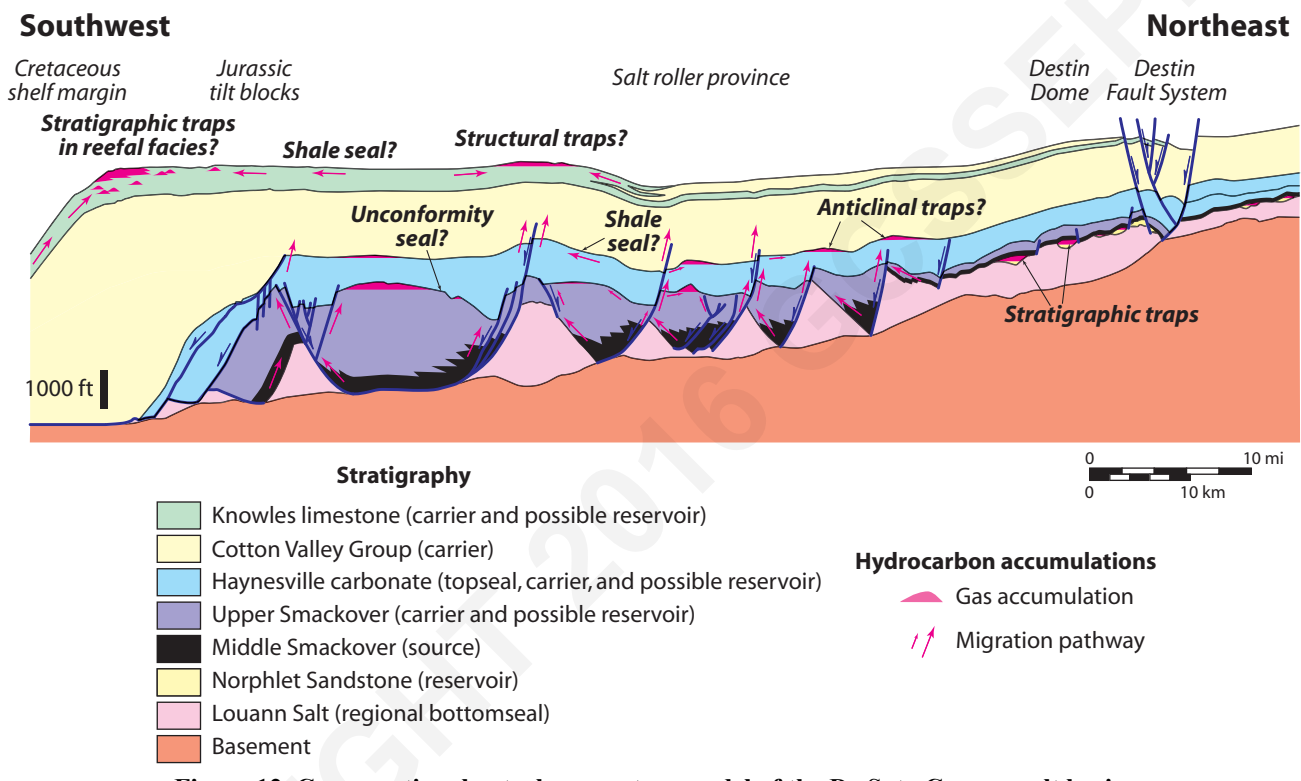


Figure 12. Cross-sectional petroleum system model of the De Soto Canyon salt basin.

Pashin et al. 448 l

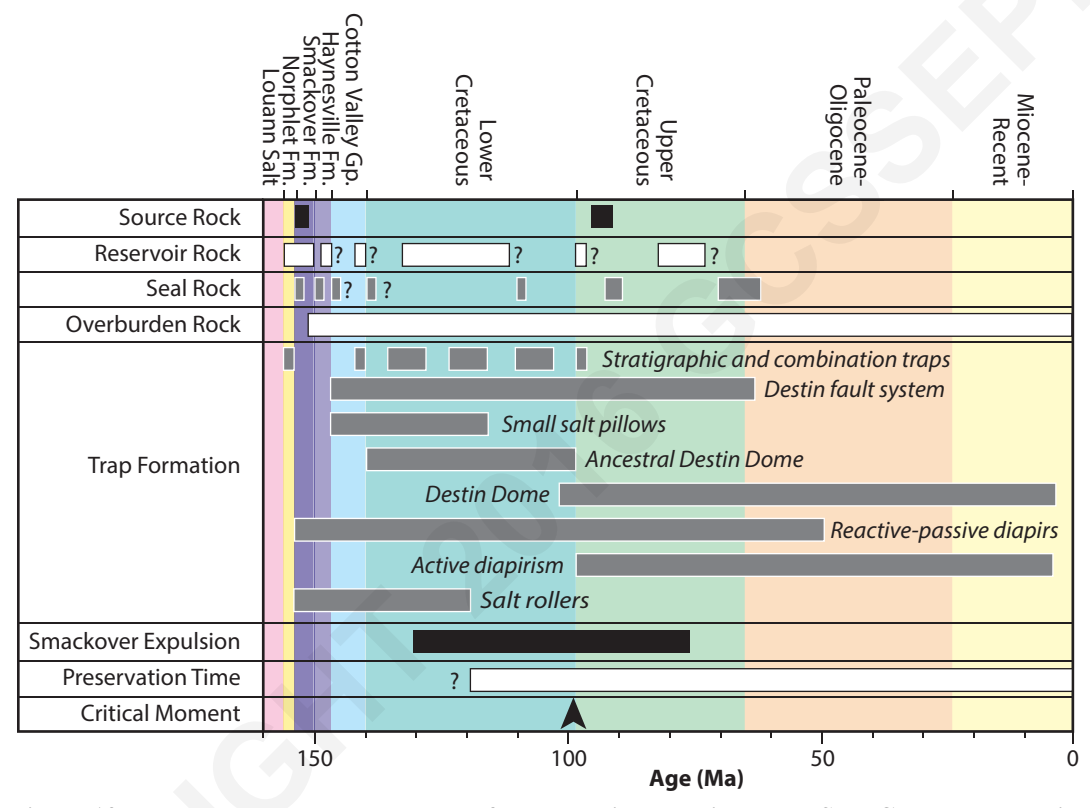


Figure 13. Petroleum systems event chart for Mesozoic strata in the De Soto Canyon salt basin.